15TH IEA HEAT PUMP CONFERENCE
MAY 26–29, 2026 | HOFBURG
VIENNA 2026
DECARBONISATION THROUGH INNOVATION

A model-based analysis of a near-adiabatic system with two high-temperature heat pumps for sustainable paper drying

Osama Ali Ahmed Awan[a,*], Johannes Lunewski[a], Toma Schneider[b], Isabel Kuperjans[c], Peter Bekaert[a]

[a]Modellfabrik Papier gGmbH, August-Klotz-Straße 21, 52349 Düren, Germany.
[b]PTS - Institut für Fasern & Papier gGmbH, Pirnaer Straße 37, 01809 Heidenau, Germany.
[c]Institute NOWUM-Energy, FH Aachen, University of Applied Sciences, Heinrich-Mussmann-Str. 1, 52428 Juelich, Germany.

Abstract

Climate change poses a significant threat to the environment, with industrial processes being among the largest contributors to the global carbon footprint. The paper industry contributes significantly to carbon emissions due to its high energy demand, with its energy mix relying on roughly one-third fossil fuels, one-third non-fossil-based sources, and one-third electricity. This highlights the urgent need for the paper industry to shift towards green and sustainable practices. The drying section is the most energy-intensive stage of the papermaking process, accounting for around 60% of total energy consumption. Therefore, there is an opportunity to reduce energy consumption and carbon emissions. This paper proposes and models the concept of a novel technology carrier, which consists of two high-temperature heat pumps operating simultaneously to create a near-adiabatic process for paper drying. The first heat pump is an open-cycle system that captures exhaust air from the drying hood and compresses it to increase its temperature. This hot, compressed air is then used for the following purposes: to act as the heat source for a second heat pump, to heat process water, to preheat incoming fresh air, and to generate electricity. The second heat pump absorbs heat from the first one and delivers steam at above 200 °C and 6 bar(a), using water as its refrigerant. The Python model is also used to investigate the following: how multistage compression with intercooling manages compressor discharge temperature in a high-temperature heat pump using water as a refrigerant, the effects of variations in moisture content and exhaust air temperature on heat recovery system performance, and potential methods for improving the heat recovery system's coefficient of performance to enhance overall efficiency. The insights presented here lay the groundwork for future research and collaboration with the paper industry, supporting the transition towards sustainability.

Keywords: Energy transition; Paper production; Energy efficiency; High-temperature heat pumps; Heat recovery; Electrification.

1. Introduction

The generation of electricity and heat from fossil fuels is associated with a significant carbon footprint, which has threatened the prosperity and sustainable development of our planet by increasing the average global temperature. As a corrective measure, around 195 signatories agreed to limit the rise in the global temperature to well below 2 °C above pre-industrial levels, while also pursuing efforts to restrict it to 1.5 °C in Paris agreement in 2015 [1]. Achieving these goals requires a fundamental shift toward greener practices in energy-intensive industries, as they account for roughly 25% of global greenhouse gas emissions. Among these industries, the pulp and paper sector alone accounts for approximately 6% of global industrial energy consumption and about 2% of industrial CO_2 emissions [2]. The energy-intensive nature of this sector is exemplified by the German paper industry, where one ton of paper produced in 2024 consumed around 2724

* Corresponding author. *E-mail address:* osama.awan@modellfabrikpapier.de

kWh of energy and emitted approximately 0.488 tons of CO_2 [3]. Therefore, the paper and pulp industry needs to implement alternative solutions to significantly reduce energy consumption and CO_2 emissions.

The papermaking process comprises several sequential operations designed to transform a dilute fiber suspension into a consolidated paper web. The process initiates with the preparation of an aqueous suspension typically containing 0.2-1.0% fiber consistency. The suspension is uniformly distributed onto a moving mesh through the headbox. During the forming section, the fiber suspension undergoes initial dewatering through gravitational drainage and an applied vacuum, creating a coherent fiber network. The web then enters the press section, where mechanical rollers apply pressure to remove a significant portion of the remaining water. Subsequently, it moves to the drying section, where the residual moisture is evaporated by passing the web through a series of steam-heated cylinders. The process concludes with calendering and rolling [4-5].

Within papermaking, the drying process accounts for approximately 60% of the total energy consumption [4]. Furthermore, the cost of removing one unit of moisture increases dramatically across the production stages; the ratio of operational, energy, and investment costs is roughly 1:5:220 for forming, pressing, and drying, respectively [6]. Table 1 illustrates the variation in dry content, share in dewatering, and relative energy consumption across the different drying stages of the papermaking process. This substantial cost and energy intensity make the drying section an important area for improvement to reduce the overall energy consumption and carbon emissions. Therefore, this work focuses on alternative solutions to reduce energy consumption and carbon emissions in the paper drying process.

Table 1. Dry content, share in dewatering, and relative energy consumption across the different drying stages of the papermaking process [4-6].

Process stage	Dry content (%)	Share in dewatering (%)	Relative energy consumption (%)
Forming	16-22	94	1-2
Pressing	40-55	4	3-10
Drying	90-96	1	88-96

The multi-cylinder drying process is the most widely used paper-drying technique, employed in approximately 85–90% of industrial paper machines [7]. Typically, the drying section consists of 35–70 rotating cylinders. This technology is a contact drying process, in which heat is transferred from steam to the paper web to evaporate water [6]. Steam characteristics, such as temperature and pressure, vary across the different groups of drying cylinders and depend significantly on the paper grade being dried. Typically, the required steam temperature and pressure for paper drying range from 90–250 °C and 3–12 bar(a), respectively [8-9]. The evaporated water from the paper web mixes with preheated air in the drying hood surrounding the cylinders. The two important characteristics of the exhaust air are its temperature and its water vapor content. The latter is expressed by the humidity ratio (x), which is the ratio of the mass of water vapor per unit mass of dry air (kg/kg). Typically, the moist air has a temperature of 82-85 °C and x of approximately 0.1 to 0.2 kg of water per kg of dry air [10]. This moist air is then directed to the heat recovery section via ventilators. In most paper machines, the moist air is used to preheat the incoming fresh air and process water using a series of heat exchangers. However, still a significant amount of heat is lost to the environment.

Currently, the steam for drying cylinders is supplied by fossil fuel-based boilers or combined heat and power (CHP) systems, which contribute to greenhouse gas emissions (GHG) emissions. High-temperature heat pumps (HTHPs) have emerged as an efficient and feasible alternative for sustainable steam generation [9, 10]. HTHPs have also proven effective for industrial heat recovery across a wide range of sectors [11-14], demonstrating their potential to capture maximum heat. Therefore, this work proposes a novel system that integrates two distinct HTHP test rigs into a single technology carrier. The first is an open-cycle heat pump designed to capture waste heat, and the second is a close-cycle heat pump that delivers steam at the required operating conditions.

Additionally, as the industry's current focus is on low global warming potential (GWP) refrigerants, this work will investigate a heat pump system using water as the refrigerant for steam generation. The primary reasons for this choice are as follows [17]:

- Zero ozone depletion potential (ODP) and a very low-GWP.
- It is non-flammable, non-toxic, and chemically inert at high temperatures.
- It is suitable for high-temperature applications due to its high critical temperature.
- The high-temperature source from the open-cycle heat recovery system mitigates the risk of ice formation for water that would occur with a low-temperature source.
- The generated steam can be used directly in the drying cylinders, which act as the condenser for the heat pump.

However, heat pumps using water as a refrigerant also face significant challenges. Disadvantages include the water's high specific volume, high polytropic exponent, and low molecular weight. These properties result in high volumetric flow rates, compression ratios, and discharge temperatures, which pose considerable technical design challenges [18]. Nevertheless, many researchers are currently exploring solutions to these problems to take advantage of the benefits of water as a refrigerant. For instance, Kilicarslan and Müller [19] compared the performance of water with other refrigerants in heat pump. They reported that water has shown a superior performance against other considered refrigerants for source temperatures above 20 °C and medium temperature lifts. However, the authors reported that more specifically designed compressors with intercooling can improve the performance of heat pumps with water as a refrigerant for higher temperature lifts. Furthermore, Wu et al. [20] conducted experiments on a HTHP test rig with steam as a refrigerant and wet compression. The authors reported that the coefficient of performance (COP) of the proposed system reduced from 6.10 to 1.96, when the sink temperature was increased from 111 °C to 150 °C. The highest COP was achieved at a source temperature of 85 °C and a sink temperature of 117 °C. The authors reported that when the temperature lifts were constant, the COP of the system improved with increase in output temperature. In another study by Wu et al. [21], a heat pump model with water as a refrigerant was developed to analyse the performance under different operating conditions. The authors reported that the system exhibited a COP ranging from 3.64 to 4.87, when the source and sink temperatures were between 83–87 °C and 120–128 °C, respectively. However, an increase in temperature lift decreased the COP of the system. Furthermore, Wu et al. [22] proposed a simulation model to analyze a new hybrid HTHP with water as the working fluid. They coupled a mechanical vapor compression heat pump with an absorption heat transformer. The proposed system was able to reach output temperatures up to 180 °C and temperature lifts up to 110 °C. Moreover, Zühlsdorf et al. [23] conducted an exergy-based analysis to compare the performance of different refrigerants and cycle configurations. The authors reported that cycle configuration significantly influences the COP of the heat pump. They also noted that the exergy destruction caused by the throttling valve can be significantly reduced through the application of an internal heat exchanger. In another study, Hu et al. [24] conducted a comprehensive thermodynamic, and economic analysis to evaluate the performance of a cascade HTHP. The authors found that approximately 62% of the total exergy destruction was avoidable. The main components resulting in low COP were the low- and high-stage compressors, accounting for 27% and 34%, respectively. Therefore, the authors emphasized the importance of improving the compressor performance to reduce the overall emissions and enhance cost efficiency. These studies collectively highlight both the potential and the challenges of using water as a refrigerant in HTHPs. The primary challenges identified include compressor design limitations, immiscibility with lubricating oils, high discharge temperatures, and a lower COP. Conversely, its significant potential lies in achieving higher temperature lifts and possessing a low GWP.

Recent research studies have extensively highlighted the significant potential for heat recovery in the paper industry. Wilk et al. [25] reported that superheated steam drying with heat recovery has the potential to reduce about 70% energy consumption and 88% CO_2 emissions compared to traditional paper drying. In another study, Bengtsson et al. [26] proposed retrofit solutions for paper and pulp industry using pinch analysis and matrix method to find the excess heat. The authors concluded that there is a significant amount of excess heat, which can either be used for pre-evaporation of effluents at low temperature or in heat pumps to deliver steam at low-pressure levels. Furthermore, Deventer [27] conducted a feasibility study to access the heat recovery potential in superheated steam drying of paper. The authors carried out the study on a small scale and recommended that heat recovery systems can be added in the paper industry and have potential to recover around 50% of the total energy input. Moreover, Godin [28] presented a model-based framework to improve energy efficiency and reducing carbon emissions of the dryer section of paper mills. They applied their model on a German paper mill, which showed significant improvement for the energy efficiency. They reported that switching to hydrogen or electricity is not a competitive solution, although it will mitigate the carbon emissions due to higher energy prices. However, they noted that this approach could become viable if the cost of electricity is less than assumed in their study. However, HTHPs could be a better option for heat recovery and steam generation.

While the aforementioned literature highlights the significant potential of HTHPs for process heat generation and waste heat recovery, their integration into the paper industry remains hindered by several research gaps. Although water as a refrigerant in HTHPs has potential to achieve high sink temperatures, the system's COP is often limited by exergy destruction and non-optimized cycle configurations. Furthermore, the effect of variable exhaust air conditions from the drying hood (e.g., temperature and humidity) on the performance and stability of the heat recovery has not been adequately addressed. Moreover, a critical gap exists in identifying the optimal system configuration for integrating HTHPs into paper drying to simultaneously recover waste heat and supplying steam at required operating conditions.

By keeping the above-mentioned research gaps, this work develops a comprehensive analytical model of a technology carrier that combines two different heat pump systems for heat recovery and steam supply, simultaneously. After the model development, the following research questions are investigated in this work:

- How can multistage compression with intercooling manage compressor discharge temperature in a HTHP with water as refrigerant to deliver steam at required conditions?
- How does the variation of water vapor content (x) and temperature of the exhaust moist air influence the performance of the heat recovery system in the proposed technology carrier?
- How can the COP of the heat recovery system be improved to enhance the overall performance of the technology carrier?

This work comprises five sections. It begins with a description of the proposed system in Section 2. Section 3 details the methodology for developing the analytical model. The results and a discussion addressing the research questions are presented in Section 4. Finally, Section 5 provides the conclusions and proposed future work. Overall, this work aims to provide critical insights for integrating HTHPs into the paper drying process, facilitating a path toward sustainable paper production.

2. System description

Figure 1 illustrates the proposed technology carrier, which integrates two distinct HTHP systems: an open cycle for heat recovery and a close-cycle with water as the refrigerant for steam supply. These are hereafter referred to as the heat recovery system (HRS) and steam supply system (SSS), respectively.

The process begins at the drying hood, where the exhaust air exits the drying section. This moist air stream is first compressed within the HRS. The compression shifts the dew point to a higher level of the exhaust air and significantly enhances its heat recovery potential compared to conventional methods. The high-pressure high-temperature exhaust air then passes through a series of heat exchangers, where the heat is recovered. The first heat exchanger serves as the source for the evaporator of the steam supply system. In the second heat exchanger, the recovered thermal energy heats up the process water that can be used for different purposes in the papermaking process. After that, the incoming fresh air for the drying section is pre-heated in the third heat exchanger. Subsequently, the air-vapor mixture passes through a condensate separator, where the condensate is removed. The pressure is then reduced by an expander, which generates power, before the stream passes through a second condensate separator. The process concludes with the release of dry air at near-ambient temperature. This system effectively maximizes energy extraction by recovering both sensible and latent heat from the exhaust stream.

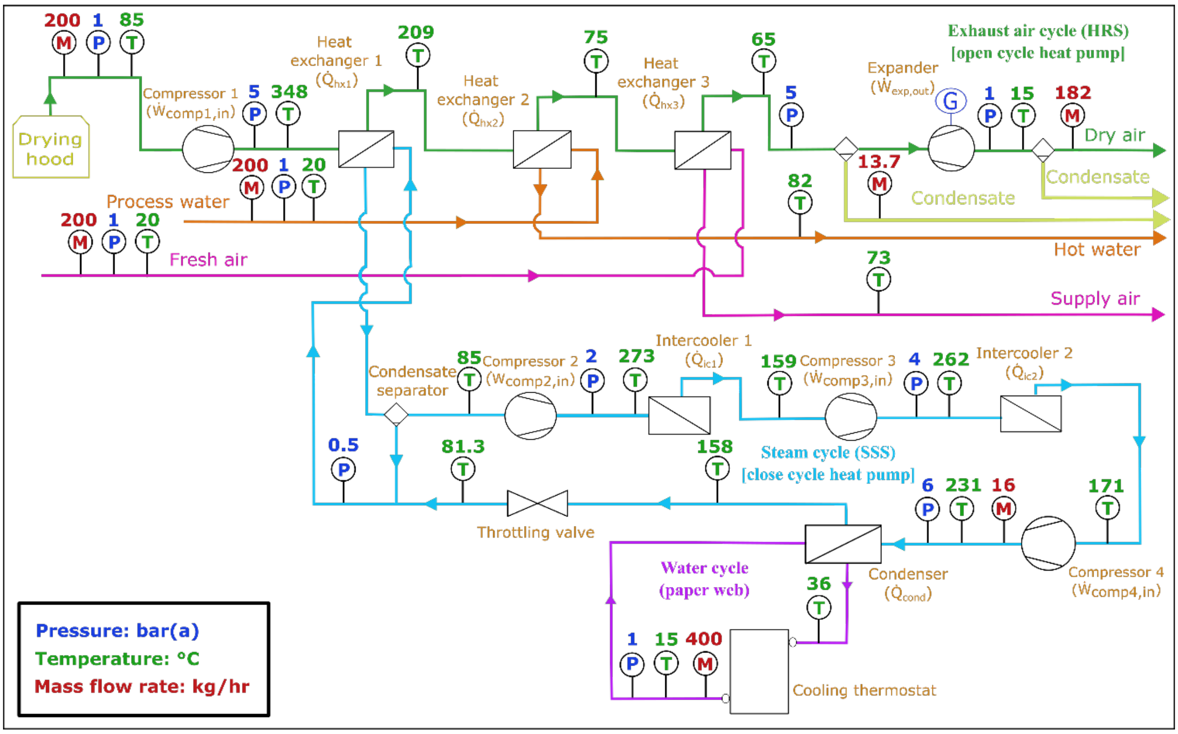

Figure 1: Schematic diagram of the proposed technology carrier consisting of two different heat pump systems.

The steam supply system utilizes the heat recovered by HRS to demonstrate a closed-cycle heat pump using water as the refrigerant. This heat pump supplies steam tailored to the required operating parameters (temperature and pressure). The cycle begins with the compression of steam from 0.5 bar(a) to 6 bar(a) via a multi-stage compression with intercooling. This configuration was selected to manage the compressor discharge temperature when the pressure is increased, as high temperature can be harmful for the components. Further details on this design choice are provided in Section 4. The high-pressure steam then enters a condenser, which simulates the heat transfer to a paper web in an industrial drying cylinder. It may be noted that no pressure drop is considered across all heat exchangers and intercoolers. After condensation, the fluid passes through a throttling valve, reducing its pressure to 0.5 bar(a). The resulting low-pressure liquid-vapor mixture then absorbs heat and vaporizes in the evaporator by absorbing thermal energy from the heat recovery system. The temperature and pressure before the first compressor are fixed at 85 °C and 0.5 bar(a) based on the analytical numerical results based on heat requirement and overall efficiency (*PTS - MFP preliminary project MFP003*) [29]. Before returning to the compressor, the fluid passes through a condensate separator, where the condensate is removed and sent back to the evaporator. This step is critical because it ensures that only dry vapor enters the compressor in order to protect the machinery. Overall, the proposed technology carrier is designed to demonstrate a near-adiabatic paper drying process, thereby minimizing thermal losses to the environment and carbon footprint.

3. Research methodology

A thermodynamic model is developed using the Python library TESPy [30], incorporating various components to represent the overall process. The CoolProp Python library is employed to obtain the thermophysical properties of different fluids used in the system modeling [31]. Since the technology carrier consists of identical components, this section describes the modeling technique for each unique component, and the same model equations is applied whenever a component is repeated. The primary components include compressor, heat exchanger, condensate separator, expander, cooler and throttling valve.

The compressor is one of the most critical components in the system. It is modelled by specifying a pressure ratio (*PR*) and an isentropic efficiency $(\eta_{\mathrm{is,comp}})$. *PR* is the ratio of outlet pressure to inlet pressure of the compressor, while $\eta_{\mathrm{is,comp}}$ is the ratio of ideal work to the actual work required by the compressor. The corresponding ideal outlet state is obtained by enforcing constant entropy between inlet and outlet. For an ideal gas with constant heat capacities, the isentropic temperature relation which provides an estimate of the isentropic outlet temperature ($T_{\mathrm{is,out}}$) is given in Equation (1).

$$T_{is,out} = T_{in}\left(\frac{p_2}{p_1}\right)^{\frac{\gamma-1}{\gamma}} \tag{1}$$

where $\gamma = c_{\mathrm{p}}/c_{\mathrm{v}}$ is the heat-capacity ratio, c_{p} and c_{v} are specific heats at constant pressure and volume, respectively, and p_1 and p_2 are the inlet and outlet pressures of the compressor. The isentropic efficiency of the compressor ($\eta_{\mathrm{is,comp}}$) is defined as the ratio of the ideal enthalpy difference to the actual enthalpy rise as given in Equation (2).

$$\eta_{is,comp} = \frac{h_{is,out}-h_{in}}{h_{a,out}-h_{in}} \tag{2}$$

where h_1 is the inlet enthalpy, $h_{\mathrm{is,out}}$ is isentropic outlet enthalpy, and $h_{\mathrm{a,out}}$ is actual outlet enthalpy. Rearranging Equation (2) gives the expression for the actual outlet enthalpy, which TESPy solves together with the compressor input power ($\dot{W}_{\mathrm{comp,in}}$). Furthermore, Equation (3) gives the power input ($\dot{W}_{\mathrm{comp,in}}$) for the compressor using the given compressor isentropic efficiency $(\eta_{\mathrm{is,comp}})$.

$$\dot{W}_{comp,in} = \frac{\dot{m}(h_{is,out}-h_{in})}{\eta_{is,comp}} \tag{3}$$

Heat exchangers are modelled in TESPy using the user-specified parameter *UA* (W/K), which is the product of the overall heat-transfer coefficient (*U*) and the effective heat-transfer area (*A*). No fixed constants are assumed; the value of *UA* is provided by the user, and thermophysical properties (e.g., enthalpy) are evaluated with CoolProp at the respective operating pressures and temperatures. The driving force for heat transfer is represented by the logarithmic mean temperature difference (LMTD), given in Equation (4).

$$LMTD = \frac{\Delta T_A - \Delta T_B}{ln\,(\Delta T_A / \Delta T_B)} \tag{4}$$

where ΔT_{A} and ΔT_{B} are the terminal temperature differences between the hot and cold streams at the two ends of the counterflow heat exchanger (hot-in minus cold-out, and hot-out minus cold-in, respectively). For known heat transfer rate ($\dot{Q}$) and terminal temperatures, *UA* can be calculated by using Equation (5).

$$UA = \frac{\dot{Q}}{\Delta T_{LMTD}} \tag{5}$$

In order to prevent liquid droplets entering the compressor and expander, condensate separators are positioned upstream of these components. This is because liquid droplets can cause erosion and component damage. The condensate separators are not available as built-in components in TESPy. Therefore, they are modelled separately in Python and then used in model. The output of the condensate separator is fixed at vapor quality of 1. Fluid expands through the expander, resulting in a pressure decrease and the generation of power. The TESPy library models this process with its 'Expander' component. Assuming steady state, adiabatic operation, the power output from expander ($\dot{W}_{\mathrm{exp,out}}$)is obtained from Equation (6).

$$\dot{W}_{exp,out} = \eta_{is,exp}\dot{m}(h_{in} - h_{is,out}) \tag{6}$$

Where $\eta_{\mathrm{is,exp}}$ is the isentropic efficiency of expander, and h_{in} and h_{out} are the specific enthalpies at the expander inlet and outlet, respectively. Between the compression stages, 'SimpleHeatExchanger' components of TESPY library are used to model intercoolers that remove heat between steam compression steps to reduce the output temperature in multi-stage compression. These intercoolers reject a prescribed amount of heat (Q) at constant pressure. The heat balance for these intercoolers is given in Equation (7).

$$\dot{Q} = \dot{m}(h_{out} - h_{in}) \tag{7}$$

where $\dot{m}$ is the mass flow rate of the working fluid (steam), and h_{in} and h_{out} are the specific enthalpies at the inlet and outlet of the intercooler, respectively. TESPy enforces the specified pressure ratio for the cooler while solving for the outlet enthalpy. The thermophysical properties, including enthalpy and temperature, are evaluated using CoolProp library. After condensation, the refrigerant is expanded through a throttling valve to reduce its pressure and temperature in order to prepare it to absorb heat from the source in the next cycle. The throttling valve is modelled in TESPy using the 'Valve' element. The throttling valve is modelled by an isenthalpic (Joule–Thomson) process in which the fluid experiences a pressure drop from the condenser pressure to the evaporator inlet pressure, while maintaining constant specific enthalpy i.e. $h_{\mathrm{in}} = h_{\mathrm{out}}$.

TESPy employs CycleCloser component to connect the terminal point of a thermodynamic loop back to its initial state. This ensures mass and energy conservation within closed cycles, allowing the software to maintain continuity of flow properties such as pressure, temperature, and enthalpy across loop boundaries.

For the evaluation, the COP is considered as the primary performance indicator of the proposed system. COP of a heat pump is the ratio of desired output heat transfer rate ($\dot{Q}_{\mathrm{H}}$) to the required power input ($\dot{W}_{\mathrm{net,in}}$). The expression to calculate COP is given in Equation (8) [32].

$$COP = \frac{\dot{Q}_H}{\dot{W}_{net,in}} \tag{8}$$

There are three different COP values that are relevant when assessing the performance of the proposed system. The first one is the COP for heat recovery system (COP_{HRS}). Since useful heat is available as the heat output from the three heat exchangers in the HRS, the total heat transfer rate ($\dot{Q}_{\mathrm{H,HRS}}$) is the sum of the heat transfer rates from these exchangers that is $\dot{Q}_{\mathrm{H,HRS}} = \dot{Q}_{hx1} + \dot{Q}_{hx2} + \dot{Q}_{hx3}$. Additionally, the expander also produces power output ($\dot{W}_{\mathrm{exp,out}}$), which needs to be subtracted from the compressor input power ($\dot{W}_{\mathrm{comp1,in}}$) to calculate the $\dot{W}_{\mathrm{net,in,HRS}}$. Equation (9) gives the expression for calculating $\dot{W}_{\mathrm{net,in,HRS}}$ [32].

$$\dot{W}_{net,in,HRS} = \dot{W}_{comp1,in} - \dot{W}_{exp,out} \tag{9}$$

It is important to mention that there are also two condensate streams from the HRS. However, their mass flow rates are small. Therefore, for simplification they are not included in the calculations. When included, they can change the COP of the system by <1%. Equation (10) gives the expression to calculate COP_{HRS} [32].

$$COP_{HRS} = \frac{\dot{Q}_{H,HRS}}{\dot{W}_{net,in,HRS}} = \frac{\dot{Q}_{hx1} + \dot{Q}_{hx2} + \dot{Q}_{hx3}}{\dot{W}_{comp1,in} - \dot{W}_{exp,out}} \tag{10}$$

For the steam supply system, when three-stage compression with intercooling is considered then the COP is calculated by Equation (11). Since there is no expander in the SSS, the $\dot{W}_{\text{net,in,SSS}}$ is the sum of work input of the three compressors that is $\dot{W}_{\text{net,in,SSS}} = \dot{W}_{comp2,in} + \dot{W}_{comp3,in} + \dot{W}_{comp4,in}$.

$$COP_{SSS} = \frac{\dot{Q}_{H,SSS}}{\dot{W}_{net,in,SSS}} = \frac{\dot{Q}_{cond}}{\dot{W}_{comp2,in} + \dot{W}_{comp3,in} + \dot{W}_{comp4,in}} \tag{11}$$

where $\dot{Q}_{\text{cond}}$ is the heat transfer rate from condenser, while $\dot{W}_{\text{comp2,in}}$, $\dot{W}_{\text{comp3,in}}$ and $\dot{W}_{\text{comp4,in}}$ are the compressor input powers. It may be noted that the heat losses from the intercoolers, $\dot{Q}_{\text{ic1}}$ and $\dot{Q}_{\text{ic2}}$, are excluded from the COP calculation as this heat is dissipated to the environment. However, if the heat is used then the COP of the SSS will increase. During analysis, for single-stage compression with no intercooling: $\dot{W}_{\text{comp3,in}} = 0$, and $\dot{W}_{\text{comp4,in}} = 0$ in Equation (11). Furthermore, for two-stage compression with one intercooler, $\dot{W}_{\text{comp4,in}} = 0$ in Equation (11). The COP of the technology carrier with two heat pumps is given in Equation (12).

$$COP_{COM} = \frac{\dot{Q}_{hx1} + \dot{Q}_{hx3} + \dot{Q}_{cond}}{(\dot{W}_{comp1,in} - \dot{W}_{exp,out}) + (\dot{W}_{comp2,in} + \dot{W}_{comp3,in} + \dot{W}_{comp4,in})} \tag{12}$$

where, as mentioned before, the second heat exchanger in HRS acts as the evaporator for the SSS; therefore, Q_{hx2} not included as useful heat in the combined COP calculation. After developing the analytical model, it is validated against the mathematical solution. The design points are then used to formulate a base case against the other results are evaluated. For the base case, the process is initiated with exhaust air having $x = 0.11$, temperature of 85 °C, and a mass flow rate of 200 kg hr^{-1}. A fixed value for the exhaust air mass flow rate is assumed as a baseline input to the model. Furthermore, the inlet conditions for incoming fresh air and process water are fixed at mass flow rate of 200 kg hr^{-1} and pressure of 1 bar(a). For the steam supply system, the closed loop is initialized at the compressor inlet with pressure of 0.5 bar(a) and mass flow rate of 200 kg hr^{-1}. In the steam-supply system, three-stage compression with intercooling is employed with pressure ratios PR_1 =4, PR_2 =2, and PR_3 =1.5 for compressors in series. These *PR* values are chosen to limit the increase in discharge temperature. A high *PR* would result in an excessively high discharge temperature, which is harmful for system components. Conversely, a low PR would result in technical complexities. For the first and second intercoolers, the prescribed duties are $\dot{Q}_{\text{ic1}}$=1 kW and $\dot{Q}_{\text{ic2}}$=0.8 kW (heat is rejected at temperatures between 250 °C and 280 °C from the stream and can be used for a secondary purpose, such as process water heating.). In the condenser, the hot side outlet is fixed to saturated liquid. At the compressor inlet, the steam is maintained at a dry saturated vapor state (x=1) to prevent the ingestion of liquid droplets. The isentropic efficiency of all considered compressors and expander is $\eta_{is} = 0.75$. For the base case, the COP_{HRS}, COP_{SSS}, and COP_{COM} are found to be 2.53, 3.34, and 1.97, respectively.

4. Results and discussion

This section presents the results and discussion for the research questions outlined in the introduction, beginning with why multi-stage compression with intercooling is considered for the steam supply system instead of single-stage compression. This also follows with an additional question, what is the optimum number of compression stages for the proposed system. The response to these questions is driven by the system's primary objective, which is to extract heat from HRS and upgrade it to deliver steam at approximately 200 ℃ and 6 bar(a). Achieving this requires a high-temperature lift of around 110-115 K and a pressure ratio of 12 in the system. However, such a high *PR* results in a very high discharge temperature, which is dangerous for the compressor and downstream components. Furthermore, it is also important to know how it affects the COP_{SSS}. A comparative study is conducted to analyze the performance of single-stage compression, two-stage compression with one intercooler, and three-stage compression with two intercoolers. In the multi-stage configurations, an intercooler is added to reduce the temperature before the next compressor. Using a single compressor to increase the pressure from 0.5 bar(a) to 6 bar(a) results in an output temperature of approximately 460.9 ℃, and a COP_{SSS} of 3.67. In the two-stage system, the pressure is increased from 0.5 bar(a) to 3 bar(a) and then to 6 bar(a), yielding a temperature of 338.1 ℃ and 230 ℃ after the first and second compressor, respectively. The intercooler in two-stage compression system reduces the temperature from 338.1 ℃ to 133.5 ℃. Furthermore, the COP_{SSS} is found to be 3.33. The three-stage configuration incorporates three compressors to increase pressure from 0.5 to 2 bar(a), 2 to 4 bar(a), and finally 4 to 6 bar(a). The resulting discharge temperatures after the first, second, and third compressors are 272.9 °C, 261.6 °C, and 231.05 °C, respectively. First and second intercooler reduce the temperature from 272.9 °C to 158.7 °C and 261.6 °C to 171.0 °C, respectively. Additionally, the three-stage compression system achieves the COP_{SSS} of 3.34. Moreover, when the compression stages are increased to four with three intercoolers, while maintaining a similar condenser inlet temperature as the three-stage system, the system COP decreases to 3.23.

The analysis results show a trade-off between operational feasibility in term of compressor discharge temperature and thermodynamic performance. While the single-stage compression system achieves a higher COP_{SSS} than multi-stage compression systems, this configuration produces very high discharge temperatures that pose a risk to compressor integrity, including oil degradation, increased thermal expansion, and high mechanical stress. Additionally, this much higher compressor discharge temperature is a potential hazard for the downstream components. In contrast, the multi-stage compression systems effectively reduce the discharge temperature. Although the COP_{SSS} for single-stage compression configuration is higher than multi-stage compression systems, the present analysis does not account for the heat rejected by the intercoolers. If the waste heat from intercoolers is recovered for industrial needs like process water heating, the COP_{SSS} for the two-stage and three-stage systems rises to 3.93 and 3.96, respectively, thereby surpassing the performance of the single-stage compression system. In addition to that, the COP_{SSS} of three stage compression system is slightly more than the two-stage compression. Furthermore, the discharge temperature after the first compressor in two-stage compression is 357.15 °C, which could also damage the compressor and downstream components. Moreover, the four-stage system was suboptimal, as its marginal thermal benefit is outweighed by a lower COP_{SSS} of 3.23, increased CAPEX costs, and greater system complexity. Consequently, based on the resulting COP_{SSS} and compressor discharge temperature, the three-stage compression system with two intercoolers is selected for this model, as it successfully delivers steam at the required pressure while maintaining safe operating temperatures and achieving the appropriate COP for the given temperature lift and pressure ratio. Figure 2 shows the comparison of pressure and discharge temperature at different stages for the systems considered, along with their respective COP_{SSS}.

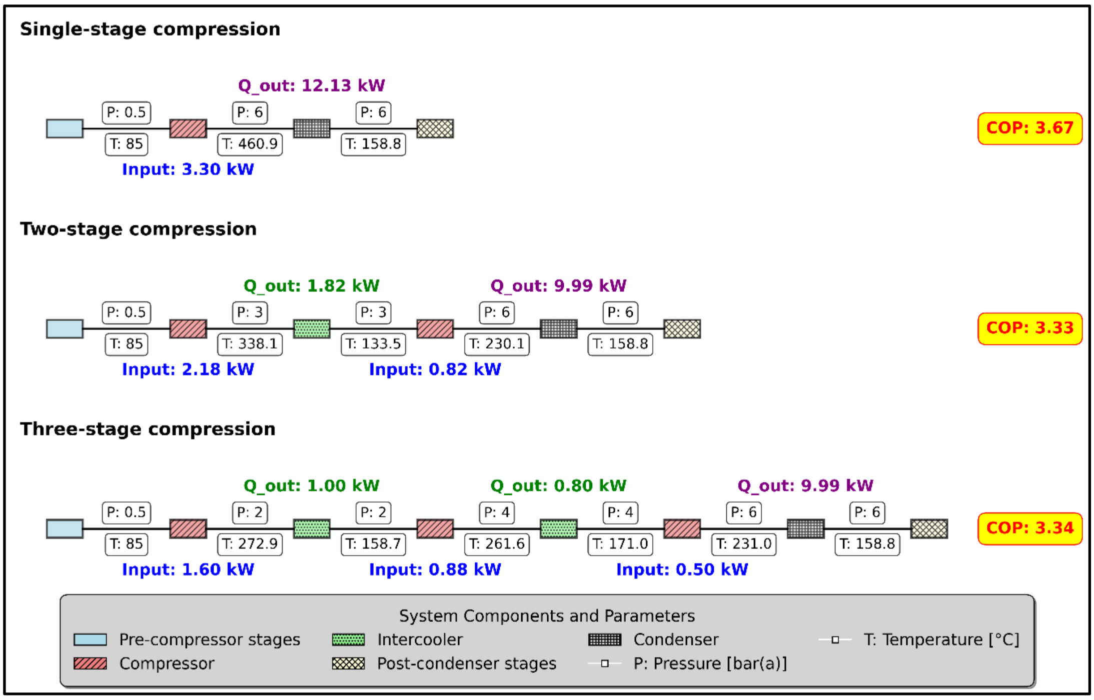

Figure 2: The comparison of discharge outlet temperature and COP_{SSS} for different configurations of steam supply system.

Next, the effect of the exhaust air characteristics on the system's performance is investigated. As mentioned earlier, the two key properties of the exhaust air are its temperature and water vapor content (x), both of which influence the COP of the heat recovery system. The water vapor content in the exhaust air originates from the evaporation of water from the paper web, which itself depends on the absorbed water content in different paper grades. Therefore, this work investigates the impact of varying x and temperature of the exhaust air on the COP_{HRS} of the proposed system. In this regard, a parametric study is conducted using six different values of x (0.11 to 0.27) and five different temperature levels (80 to 100 °C). Since the values of other parameters are kept constant, only COP_{HRS} is considered for comparison. The data in Figure 3 illustrates that a temperature increase results in a change of under 1% in COP_{HRS}, demonstrating its near-constant behavior across all values of x. This indicates that the exhaust air temperature does not have a significant influence on the system's COP. Although the output power from the expander ($\dot{W}_{exp,out}$) increases with the exhaust air temperature, the compressor's input power ($\dot{W}_{\mathrm{comp1,in}}$) also increases. Consequently, the COP remains almost unchanged or with small difference. In contrast, variations in the value of x have a significant impact on COP_{HRS}. A maximum COP_{HRS} is achieved at x =0.27, which is nearly 37% higher than the base case. The primary reason for this performance improvement is the rise in the dew point temperature of the exhaust air. In paper drying hoods, effective heat recovery depends on capturing vapors and the dew point of the captured air. A higher water vapor content (x) leads to a higher dew point, which in turn reduces steam and power consumption. Furthermore, higher water vapor content (x) also reduces the compression of unnecessary air. The key mechanism is condensation: when the heat exchanger's surface temperature falls below this elevated dew point, water vapor condenses. This process releases latent heat that can be recovered without additional electrical input, thereby increasing the system's COP. However, in practice, the moisture content (x) cannot be increased indefinitely because the resulting higher dew points lead to two significant operational risks: difficulties in manually collecting paper fragments in the event of web breaks, and an increased risk of corrosion to machine fabrics and components. The overall average achievable dew point is approximately 65 °C, though local dew points inside the hood can reach up to 75 °C [33]. Extracting this high-humidity air at local points is limited by multiple factors, including the number of extraction points, resistance from fabric contamination, and varying product types. Furthermore, the application of local extraction systems (e.g., pocket ventilators, fabric cleaners, stabilizers) is often constrained by a lack of space in existing machinery. Overall, the results demonstrate that x has a substantial influence on the heat pump's performance, whereas the effect of exhaust air temperature is almost negligible.

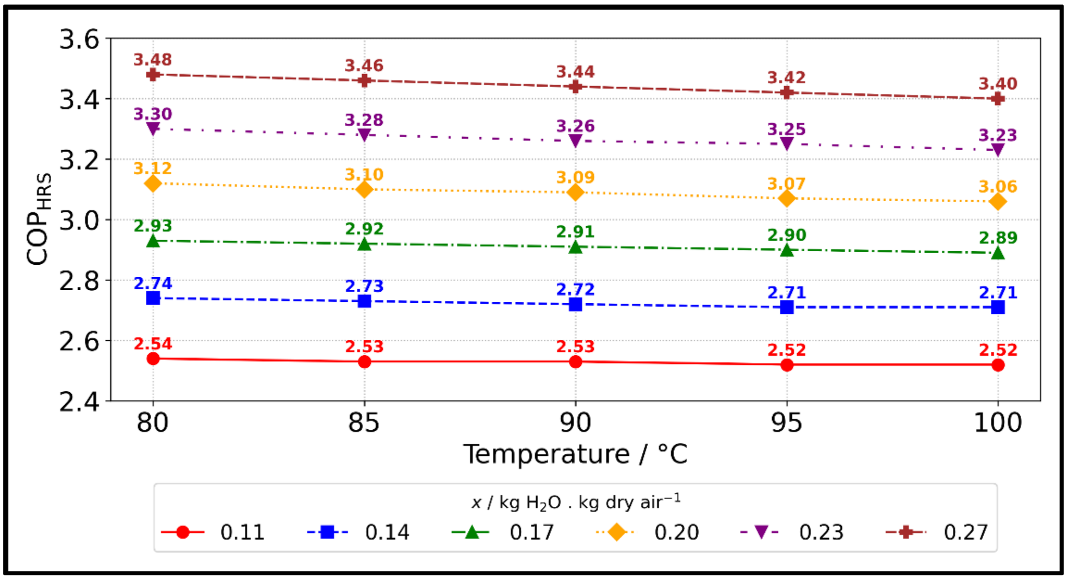

Figure 3: The resulting COP_{HRS} at different values of water vapor content x and exhaust air temperature.

A key objective of this study is to improve the COP_{HRS} and COP_{COM} of the proposed system. As mentioned above, the efficiency of all compressors and the expander in the system is considered as 75%. However, since technology advancement has resulted in more efficient components, the isentropic efficiencies of compressor ($\eta_{\mathrm{is,comp}}$) and expander ($\eta_{\mathrm{is,exp}}$) within the heat recovery system (HRS) are varied independently to analyze their effect on the overall performance. Figure 4 illustrates the comparison of COP_{HRS} and COP_{COM} with variations in compressor and expander efficiencies. Increasing the isentropic efficiency (η_{is}) of both components enhances the system's performance. When the η_{is} of both the compressor and expander is the same, the increase from 75% to 85% enhances the COP_{HRS} and COP_{COM} from 2.53 to 3.12 and 1.96 to 2.26, respectively. Furthermore, the analysis showed that higher compressor efficiency lowers the exit temperature, thereby reducing the amount of heat available for the process water, while delivering a constant amount of heat for fresh air and SSS. Furthermore, varying only the expander efficiency while keeping the compressor's efficiency constant resulted in a marginal improvement, demonstrating that the compressor has a greater effect on system performance than the expander. Consequently, a dual-stage compression cycle with intercooling is investigated to find if there is an increase in the performance of the system. This configuration replaces the single-stage compressor (compressor 1 in Figure 1) with two compressors (1a and 1b) and an intercooler. Both the compressors operate at 75% efficiency. In the first stage, exhaust air is compressed from 1 bar(a) to 3 bar(a), raising its temperature from 85 °C to 233.9 °C. An intercooler then recovers this heat to warm the incoming fresh air, cooling the exhaust stream to 156.4 °C. Subsequently, the second stage compresses the air from 3 bar(a) to the final 5 bar(a), resulting in a discharge temperature of 290.6 °C. A dual-stage compression HRS increase the COP_{HRS} and COP_{COM} by approximately 5-13%, highlighting the need to further investigate and identify the optimum cycle configuration for the heat recovery system.

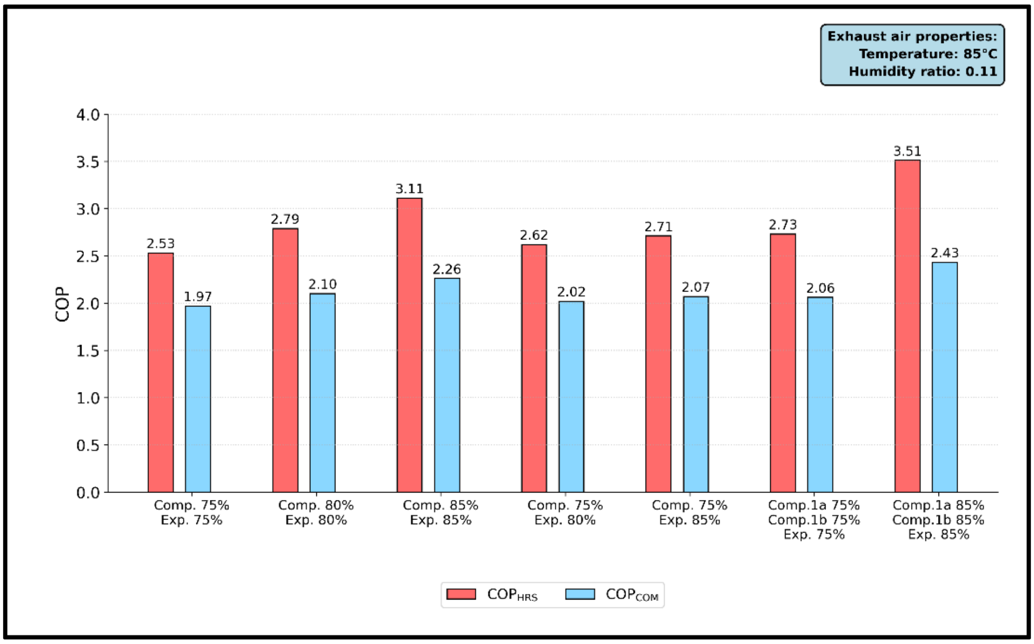

Figure 4: The comparison of performance of the heat recovery system at different efficiencies of compressor and expander.

5. Conclusions and future work

The following are main conclusions of the current research study:

- Keeping in view the desired steam sink conditions of around 200 °C and 6 bar(a) with a temperature lift of around 110-115 K and pressure ratio of 12, multi-stage compression with intercooling proves to be an effective approach for controlling the discharge temperature. This approach effectively manages the discharge temperature, preventing potential damage to the compressor and downstream components. Although the calculation shows a higher COP_{SSS} for single-stage compression than for multi-stage systems, this does not account for the heat lost from the intercoolers to the environment in multi-stage systems. When this heat loss is included, the corrected COP_{SSS} of the three-stage compression system with intercooling is approximately 8% and 14% higher than that of the two-stage and single-stage configurations, respectively. Furthermore, increasing the number of compressors to four with three intercoolers in multi-stage configurations does not improve the COP. Consequently, based on the compressor discharge temperature and COP_{SSS}, three-stage compression with two intercoolers is selected.
- Increasing the water vapor content (x) of the exhaust air significantly increases the COP_{HRS} of the system, while the exhaust air temperature does not have any substantial impact on the performance. Compared to the base case with x=0.11, increasing the x to 0.27 enhances the system's COP_{HRS} by nearly 37%.
- There is a significant improvement in the HRS performance, when the isentropic efficiency of the compressor ($\eta_{\text{is,comp}}$) and expander ($\eta_{\text{is,exp}}$) in the heat recovery system are increased. However, the compressor has more influence on the system's COP_{HRS} and COP_{COM} than the expander. Furthermore, dual-stage compression with intercooling in heat recovery system improves the COP_{HRS} and COP_{COM} by approximately 5-13% as compared to single-stage compression.

Although the analytical results provide valuable insights, experimental validation is essential to verify the system's COP. This need arises from the idealizations employed in the model, and future work should quantify their impact on the predicted COP. As a first step, a small-scale demonstration setup would be developed, incorporating two HTHP test rigs equipped to measure the pressure, mass flow rate, and temperature accurately. Furthermore, since the COP is influenced by multiple factors, it is crucial to identify which components have the greatest impact. A detailed parametric study would therefore be conducted to optimize the performance of the proposed system. Furthermore, single-stage compression such as screw compressor with water injection will be investigated to determine its effectiveness in managing discharge temperature.

Nomenclature

Latin symbols

Symbols	*Unit*	*Description*
A	m^2	Effective heat-transfer area
c	$kJ.\ kg^{-1}.\ K^{-1}$	Specific heat capacity
h	$kJ.\ kg^{-1}$	Specific enthalpy
$\dot{m}$	$kg.\ hr^{-1}$	Mass flow rate
p	bar(a)	Pressure
$\dot{Q}$	kW	Heat transfer rate
s	$kJ.\ kg^{-1}.\ K^{-1}$	Specific entropy
t	s	Time
T	°C	Temperature
ΔT	K	Temperature difference
U	$W.\ m^{-2}.\ K^{-1}$	Overall heat transfer coefficient
$\dot{W}$	kW	Power
x	$kg \cdot kg^{-1}$	Humidity ratio

Greek symbols

Symbol	*Unit*	*Description*
γ	–	Heat capacity ratio
η	–	Efficiency
ρ	$kg \cdot m^{-3}$	Density

Subscripts

Symbol	*Description*
a	Actual
comp	Compressor
cond	Condenser
COM	Combined
exp	Exapnder
hx	Heat exchanger
HRS	Heat recovery system
ic	Intercooler
is	Isentropic
SSS	Steam supply system
t	Total

Abbreviations

Abbreviation	*Description*
CHP	Combined heat and power
CO_2	Carbon dioxide
GHG	Greenhouse gas
GWP	Global warming potential
HTHP	High-temperature heat pump
ODP	Ozone depletion potential
P&ID	Piping and instrumentation diagram
PR	Pressure ratio

Acknowledgements

The authors acknowledge the support of the Forschungscluster Modellfabrik Papier (FOMOP), funded by the Federal Ministry of Research, Technology and Space, Grant Number 03STG011A.

References

[1] United Nations, “The Paris Agreement.” 2015.

[2] D. D. Furszyfer Del Rio *et al.*, “Decarbonizing the pulp and paper industry: A critical and systematic review of sociotechnical developments and policy options,” *Renewable and Sustainable Energy Reviews*, vol. 167, p. 112706, Oct. 2022, doi: 10.1016/j.rser.2022.112706.

[3] DIE PAPIERINDUSTRIE e.V., *PAPIER 2025 – Ein Leistungsbericht*. Berlin, 2025.

[4] P. Bajpai, *Pulp and paper industry: energy conservation*. Amsterdam: Elsevier, 2016.

[5] P. Bajpai, *Biotechnology for Pulp and Paper Processing*. Singapore: Springer Singapore, 2018. doi: 10.1007/978-981-10-7853-8.

[6] M. Karlsson, *Papermaking Part 2, Drying*, 2nd ed. in Papermaking science and technology. Paper Engineers’ Association/ Paper ja Puu Oj, 2010.

[7] J. Laurijssen, F. J. De Gram, E. Worrell, and A. Faaij, “Optimizing the energy efficiency of conventional multi-cylinder dryers in the paper industry,” *Energy*, vol. 35, no. 9, pp. 3738–3750, Sep. 2010, doi: 10.1016/j.energy.2010.05.023.

[8] K. Hamid *et al.*, “Potential evaluation of integrated high temperature heat pumps: A review of recent advances,” *Applied Thermal Engineering*, vol. 230, p. 120720, Jul. 2023, doi: 10.1016/j.applthermaleng.2023.120720.

[9] D. Wu, B. Hu, and R. Z. Wang, “Vapor compression heat pumps with pure Low-GWP refrigerants,” *Renewable and Sustainable Energy Reviews*, vol. 138, p. 110571, Mar. 2021, doi: 10.1016/j.rser.2020.110571.

[10] M. Karlsson, "Drying of paper—an overview: The state of paper drying knowledge," in *12th Fundamental Research Symposium*, Oxford, 2001.

[11] Y. Kim, J. Lim, H. Cho, and J. Kim, "Novel mechanical vapor recompression-assisted evaporation process for improving energy efficiency in pulp and paper industry," *Intl J of Energy Research*, vol. 46, no. 3, pp. 3409–3427, Mar. 2022, doi: 10.1002/er.7390.

[12] D. Flórez-Orrego, M. E. R. Domingos, and F. Maréchal, "Techno-economic and environmental analysis of high temperature heat pumps integration into industrial processes: The ammonia plant and pulp mill cases," *Sustainable Energy Technologies and Assessments*, vol. 60, p. 103560, 2023.

[13] A. Butean, J. Enriquez, A. Matei, A. Rovira, R. Barbero, and S. Trevisan, "A digital twin concept for optimizing the use of high-temperature heat pumps to reduce waste in industrial renewable energy systems," in *Procedia Computer Science*, 2024, pp. 123–128.

[14] X. Ma, Y. Wu, Y. Du, C. Zhang, B. Lei, and Y. Lu, "Comprehensive performance evaluation of steam generating heat pumps for industrial waste heat recovery," *Carbon Neutrality*, vol. 3, no. 1, p. 35, 2024.

[15] D. Ma, Y. Sun, S. Ma, G. Li, Z. Zhou, and H. Ma, "Study on the working medium of high temperature heat pump suitable for industrial waste heat recovery," *Applied Thermal Engineering*, vol. 236, p. 121642, 2024.

[16] H. Becker, F. Maréchal, and A. Vuillermoz, "Process integration and opportunities for heat pumps in industrial processes," *International Journal of Thermodynamics*, vol. 14, no. 2, pp. 59–70, 2011.

[17] M. Chamoun, R. Rulliere, P. Haberschill, and J. F. Berail, "Dynamic model of an industrial heat pump using water as refrigerant," *International Journal of Refrigeration*, vol. 35, no. 4, pp. 1080–1091, 2012.

[18] A. Zini, L. Socci, G. Vaccaro, A. Rocchetti, and L. Talluri, "Working Fluid Selection for High-Temperature Heat Pumps: A Comprehensive Evaluation," *Energies*, vol. 17, no. 7, p. 1556, 2024.

[19] A. Kilicarslan and N. Müller, "A comparative study of water as a refrigerant with some current refrigerants," *International Journal of Energy Research*, vol. 29, no. 11, pp. 947–959, 2005.

[20] D. Wu, J. Jiang, B. Hu, and R. Z. Wang, "Experimental investigation on the performance of a very high temperature heat pump with water refrigerant," *Energy*, vol. 190, p. 116427, Jan. 2020, doi: 10.1016/j.energy.2019.116427.

[21] D. Wu, H. Yan, B. Hu, and R. Z. Wang, "Modeling and simulation on a water vapor high temperature heat pump system," *Energy*, vol. 168, pp. 1063–1072, Feb. 2019, doi: 10.1016/j.energy.2018.11.113.

[22] D. Wu, J. Wei, and R. Z. Wang, "Performance investigation of a new hybrid high-temperature heat PUMP with natural water medium," *Energy*, vol. 314, p. 134339, Jan. 2025, doi: 10.1016/j.energy.2024.134339.

[23] B. Zühlsdorf, J. K. Jensen, and B. Elmegaard, "Exergy-based analysis of irreversibilities for heat pump working fluids and cycle layouts," *International Journal of Exergy*, vol. 35, no. 2, pp. 173–194, 2021.

[24] X. Hu, C. Shi, Y. Liu, X. Fu, T. Ma, and M. Jin, "Advanced Exergy and Exergoeconomic Analysis of Cascade High-Temperature Heat Pump System for Recovery of Low-Temperature Waste Heat," *Energies*, vol. 17, no. 5, p. 1027, Feb. 2024, doi: 10.3390/en17051027.

[25] V. Wilk, S. B. Knöttner, G. Drexler-Schmid, and T. Barz, "Superheated steam drying for paper production: process efficiency assessment," in *Proceedings of ECOS 2023: 36th International Conference on Efficiency, Cost, Optimization, Simulation and Environmental Impact of Energy Systems*, 2023, pp. 1411–1421.

[26] C. Bengtsson, R. Nordman, and T. Berntsson, "Utilization of excess heat in the pulp and paper industry—a case study of technical and economic opportunities," *Applied Thermal Engineering*, vol. 22, no. 9, pp. 1069–1081, 2002.

[27] H. C. Van Deventer, "Feasibility of energy efficient steam drying of paper and textile including process integration," *Applied Thermal Engineering*, vol. 17, no. 8–10, pp. 1035–1041, 1997.

[28] H. Godin and P. Radgen, "Model-based framework for the evaluation of energy-efficiency measures in multi-cylinder paper drying," *Drying Technology*, vol. 40, no. 13, pp. 2723–2740, Oct. 2022, doi: 10.1080/07373937.2021.1958338.

[29] "Thermodynamische Optimierung des Papierherstellungsprozesses MFP-2022-P003," Jan. 08, 2024.

[30] F. Witte, I. Tuschy, and TESPy Developers, *TESPy – Thermal Engineering Systems in Python*. (2025). Accessed: Sep. 04, 2025. [Online]. Available: https://tespy.readthedocs.io

[31] CoolProp Developers, *CoolProp: Open-source thermophysical property database*. (2025). [Online]. Available: https://coolprop.org

[32] Y. A. Çengel, M. A. Boles, and M. Kanoğlu, *Thermodynamics: an engineering approach*, Ninth edition. New York, NY: McGraw-Hill Education, 2019.

[33] Voith GmbH & Co. KGaA, "Air systems for paper production." Accessed: Oct. 28, 2025. [Online]. Available: https://www.voith.com/corp-en/papermaking/air-systems.html